Received: 13 September 2016 | Accepted: 23 January 2017
DOI: 10.1002/hyp.11134

WILEY

RESEARCH ARTICLE

Bedrock geology controls on catchment storage, mixing, and release: A comparative analysis of 16 nested catchments

Laurent Pfister[1] | Núria Martínez-Carreras[1] | Christophe Hissler[1] | Julian Klaus[1] | Gwenael E. Carrer[1] | Mike K. Stewart[2] | Jeffrey J. McDonnell[3,4]

[1] Luxembourg Institute of Science and Technology, Environmental Research and Innovation Department, Catchment and Eco-hydrology Group, Belvaux, Luxembourg
[2] Geological and Nuclear Science, Lower Hutt, New Zealand
[3] Global Institute for Water Security, University of Saskatchewan, Saskatoon, Canada
[4] Northern Rivers Institute, University of Aberdeen, Scotland, UK

Correspondence
Laurent Pfister, Environmental Research and Innovation Department, Catchment and Eco-hydrology Group, Luxembourg Institute of Science and Technology, 41 rue du Brill, L-4422 Belvaux, Luxembourg
Email: laurent.pfister@list.lu

Funding information
FNR/INTER/DFG/14/02/CAOS-2 & FNR/CORE/C14/SR/8353440/STORE-AGE projects

Abstract
The bedrock controls on catchment mixing, storage, and release have been actively studied in recent years. However, it has been difficult to find neighbouring catchments with sufficiently different and clean expressions of geology to do comparative analysis. Here, we present new data for 16 nested catchments (0.45 to 410 km^2) in the Alzette River basin (Luxembourg) that span a range of clean and mixed expressions of schists, phyllites, sandstones, and quartzites to quantify the relationships between bedrock permeability and metrics of water storage and release. We examined 9 years' worth of precipitation and discharge data, and 6 years of fortnightly stable isotope data in streamflow, to explore how bedrock permeability controls (a) streamflow regime metrics, (b) catchment storage, and (c) isotope response and catchment mean transit time (MTT). We used annual and winter precipitation–run-off ratios, as well as average summer and winter precipitation–run-off ratios to characterise the streamflow regime in our 16 study catchments. Catchment storage was then used as a metric for catchment comparison. Water mixing potential of 11 catchments was quantified via the standard deviation in streamflow δD ($\sigma\delta D$) and the amplitude ratio (A_S/A_P) of annual cycles of $\delta^{18}O$ in streamflow and precipitation. Catchment MTT values were estimated via both stable isotope signature damping and hydraulic turnover calculations. In our 16 nested catchments, the variance in ratios of summer versus winter average run-off was best explained by bedrock permeability. Whereas active storage (defined here as a measure of the observed maximum interannual variability in catchment storage) ranged from 107 to 373 mm, total catchment storage (defined as the maximum catchment storage connected to the stream network) extended up to ~1700 mm (±200 mm). Catchment bedrock permeability was strongly correlated with mixing proxies of $\sigma\delta D$ in streamflow and $\delta^{18}O$ A_S/A_P ratios. Catchment MTT values ranged from 0.5 to 2 years, based on stable isotope signature damping, and from 0.5 to 10 years, based on hydraulic turnover.

KEYWORDS
bedrock permeability, catchment storage, mean transit time, mesoscale, stable isotope response, streamflow regime

1 | INTRODUCTION

Catchments exhibit three main hydrological functions: water collection (e.g., precipitation and snow), storage (across various compartments and of varying durations), and release (e.g., discharge; Black, 1997). Although we understand mechanistically the translation of intermittent delivery of precipitation into (more or less attenuated) hydrological responses (e.g., Jencso et al., 2009; Martínez-Carreras et al., 2016; McGuire & McDonnell, 2010), much of this knowledge stems from decades of research linking the storage and release of water in the thin veneer of soil to the stream signal. But catchments have much deeper storages below the soil profile, and our understanding on how these deeper storages (linked to weathered and unweathered bedrock) control water collection, storage, mixing, and release remains incomplete.

Although much work is currently underway to map and understand the critical zone (Brantley et al., 2016), past work has shown strong controls of basin geology on low flow (Smakhtin, 2001), peak flows (Onda, Komatsu, Tsujimura, & Fujihara, 2001), storage–discharge relations (Creutzfeldt et al., 2014), contaminant transport (Haria & Shand, 2004), and run-off generation (Kosugi, Katsura, Katsuyama, & Mizuyama, 2006). In the past decade, there has been progress in relating streamflow metrics to subbasin geology. Tague and Grant (2004) showed that the percentage of certain rock types in 27 subcatchments (2.8–516 km^2) draining into the 30,000-km^2 Willamette basin in Oregon could explain over 75% of the variance of summer low flow. This work built on early concepts from process understanding and headwater-scale research (Montgomery et al., 1997). More recently, Sayama, McDonnell, Dhakal, and Sullivan (2011) used seasonal water balances for 17 nested catchments of the 111.7-km^2 Elk River in Northern California to show that geology and topography together could explain over 70% of the dynamic storage changes across multiple subbasin scales.

However, the controls of geology on catchment storage, mixing, and release have been difficult to show empirically and understand mechanistically. Little of the work thus far has combined flow information with tracer information to examine storage and release holistically (with notable exceptions that we discuss below). It has also been logistically difficult to find neighbouring catchments (where inputs are similar) with sufficiently different and clean expressions of geology to do comparative analysis—as per a classic paired catchment analysis—across different neighbouring lithologies. Progress in understanding geological controls on storage and release has been further hampered by the scaling of dominant run-off processes, thus making them a moving target of sorts to pin down (Didszun & Uhlenbrook, 2008; Fröhlich, Breuer, Vaché, & Frede, 2008). Other issues have stymied progress, such as unobservable subsurface heterogeneity, sometimes boundary conditions (Beven, 2006), or the technical difficulties inherent in the direct measurement of storage at the catchment scale (Creutzfeldt et al., 2014; Tetzlaff, McNamara, & Carey, 2011; Troch et al., 2007). Moreover, storage–discharge relationships are known to be nonlinear and to exhibit hysteretic patterns (Beven, 2006; Spence, 2010). The degree of hysteresis can be controlled by antecedent storage, as well as by catchment scale (Davies & Beven, 2015).

McDonnell and Beven (2014) have recently called for a more systematic combination of hydrograph and stable isotope measurements with a view to better understand catchment storage dynamics (i.e., changes in catchment response through wetting-up and drying cycles). Tracer-based work has been essential to show strong physiographic controls on catchment-scale transport. In this context, McGuire et al. (2005) found no evidence for controls of catchment area on isotope-inferred base flow mean transit time (MTT), but instead a strong correlation between MTT and topographic indices in the western Cascade Mountains of Oregon (United States). In the granitic Strengbach catchment (0.8 km^2) in the French Vosges massif, Viville, Ladouche, and Bariac (2006) have documented geological controls on MTT. Likewise, Asano and Uchida (2012) demonstrated how the spatial distribution of base flow MTT was related to the depth of hydrologically active soil and bedrock—rather than topography—in the 4.27-km^2 Fudoji catchment in Japan. For the 749-km^2 North Esk catchment in north-east Scotland, Capell, Tetzlaff, Malcolm, Hartley, and Soulsby (2011) demonstrated with a multivariate tracer approach how hydrological and hydrochemical characteristics of two contrasting landscape types (i.e., lowlands and uplands) reflect distinct features in climate, land use, and geology.

Other basin-scale work has shown that soil type and drainage class can exert a large control on baseflow MTT (Soulsby, Tetzlaff, Rodgers, Dunn, & Waldron, 2006; Tetzlaff, Seibert, McGuire, et al., 2009; Tetzlaff, Seibert, & Soulsby, 2009) and that contrasting bedrock permeabilities can influence streamwater transit time-scaling relations (Hale & McDonnell, 2016). In a set of 20 headwater catchments in the Scottish Highlands (<1–35 km^2, grouped in seven geomorphologically and climatically distinct regions), Hrachowitz, Soulsby, Tetzlaff, Dawson, and Malcolm (2009) have regionalised Cl^--inferred MTTs through landscape (i.e., soil cover, drainage density, and topographic wetness index) and climate (precipitation intensity) controls. From the increasing evidence on physiographic controls on hydrochemical and isotopic signatures, new conceptual frameworks have recently been introduced on (time-variant) catchment (water and solute) storage and release functions (e.g., Botter, Bertuzzo, & Rinaldo, 2011; Klaus, Chun, McGuire, & McDonnell, 2015; Rinaldo et al., 2015).

Although many data points are accumulating from different geological conditions around the world, these data are difficult to compare as few places have sufficient numbers of experimental catchments on neighbouring assemblages of different basin geology to directly assess empirically the geological controls on catchment water mixing, storage, and release. Some have noted the geographical bias of this work to date (Rinaldo et al., 2015). McNamara et al. (2011) and Buttle (2016) have begun intercomparison work across sites, proposing catchment storage as a metric for comparing catchments characterised by contrasted physiographic characteristics. But as yet few examples have emerged in the literature where concept development and testing can be accomplished.

So what is the way forward? It is clear that we need to develop meaningful storage metrics for robust catchment comparison. These metrics need to characterise mixing potential of catchments across a wide range of spatial scales and physiographic settings. And to do this, we need something of a paired catchment approach where geological and physiographic characteristics can be compared and contrasted within a homogenous climate setting (as advocated by Carey et al., 2010).

Here we present a new dataset from the Alzette River basin in Luxembourg (Europe) that, we think, fulfils most of the key criteria for quantifying the controls of bedrock geology on catchment storage, mixing, and release. We leverage homogeneous climatological conditions across catchments (Pfister, Iffly, El Idrissi, & Hoffmann, 2000; Pfister, Iffly, Hoffmann, & Humbert, 2002) against distinct catchment bedrock types to test hypotheses about bedrock geology controls on fundamental catchment functions of water collection, storage, and release. We rely on 9 years of discharge and climate data in a set of 16 nested catchments (0.45 to 410 km^2), as well as fortnightly ^{18}O and D stable isotope data in precipitation and stream flow for a subset of 11 catchments. The catchments span a wide range of clean and mixed combinations of eight distinct rock types ranging from schist to marl, sandstone, dolomite, limestone, and alluvial deposits.

We examine 9 years' worth of precipitation and discharge data (for all 16 nested catchments), and 6 years of fortnightly stable isotope data in precipitation and streamflow (for a subset of 11 catchments), to investigate how bedrock geology (and resulting catchment physiography) control key elements of storage and release. Our main research questions are as follows:

1. What is the relationship between catchment bedrock geology and streamflow metrics (mean annual discharge, winter and annual precipitation–discharge ratios, and average summer/winter discharge ratios)?
2. How does bedrock geology affect water-balance-derived storage estimates, storage–discharge relationships, and seasonal storage deficit?
3. How does bedrock geology affect stream isotope response to storm rainfall and long-term damping of isotopic signatures?

2 | STUDY AREA

The 16 study catchments lie within the 1078-km^2 Alzette River basin, located in Luxembourg (Figure 1; Table 1). Catchment elevations are highest in the northern part of the Alzette basin (395 to 498 m above sea level—see Table 1), belonging to the Ardennes Massif. This area of Devonian bedrock is overlain by schists, slate, phyllites, sandstones, and quartzites (Juilleret, Iffly, Pfister, & Hissler, 2011). Periglacial deposits that mantle this area exhibit substantial porosity and may therefore also store considerable amounts of water (Juilleret et al., 2011). Similarly, previous detailed hydrogeological analysis (Martínez-Carreras et al., 2016; Wrede et al., 2015) has shown that rock weathering is considerable in the Ardennes Massif, where substantial porosity in the upper layers of otherwise compact schists, slate, and phyllites bedrock can occur. Further south, alternating layers of (permeable) sandstone and (impermeable) marls (Wrede et al., 2015) form the eastern limit of the sedimentary Paris Basin. In this cuesta landscape, catchment elevations range from 278 to 354 m above sea level.

The local climate is dominated by westerly atmospheric circulation and temperate air masses from the Atlantic (Pfister, Humbert, & Hoffmann, 2000). Seasonal differences in air temperature measured over the period 1971–2000 are 3.8 °C in winter (from October to March) to 14.3 °C in summer (from April to September). Precipitation is evenly distributed throughout the year. The spatial distribution of mean annual precipitation is slightly influenced by topography and ranges from 1100 mm along the north-western boundaries of the Alzette basin to 850 mm along its eastern border (Pfister, Wagner, Vansuypeene, Drogue, & Hoffmann, 2005).

In the Ardennes Massif, land cover is dominated by forest (mixed oak, beech, spruce, and Douglas fir forest stands) on hillslopes and a mixture of grassland and cropland on plateaus. Soils are silty, mixed with gravel, and classified as Leptosols, Cambisols, and Regosols (FAO-ISRIC-IUSS, 2006). Catchments in the sedimentary Paris Basin are dominated by alternating layers of marl, sandstone, and limestone, dipping southward and cut by rivers flowing predominantly east and northward. Sandstone and limestone outcrops are covered mainly by forests, while grassland and arable land dominate on marl substratum. Sandstone bedrock is overlain by Podzols, Luvisols, Umbrisols, and

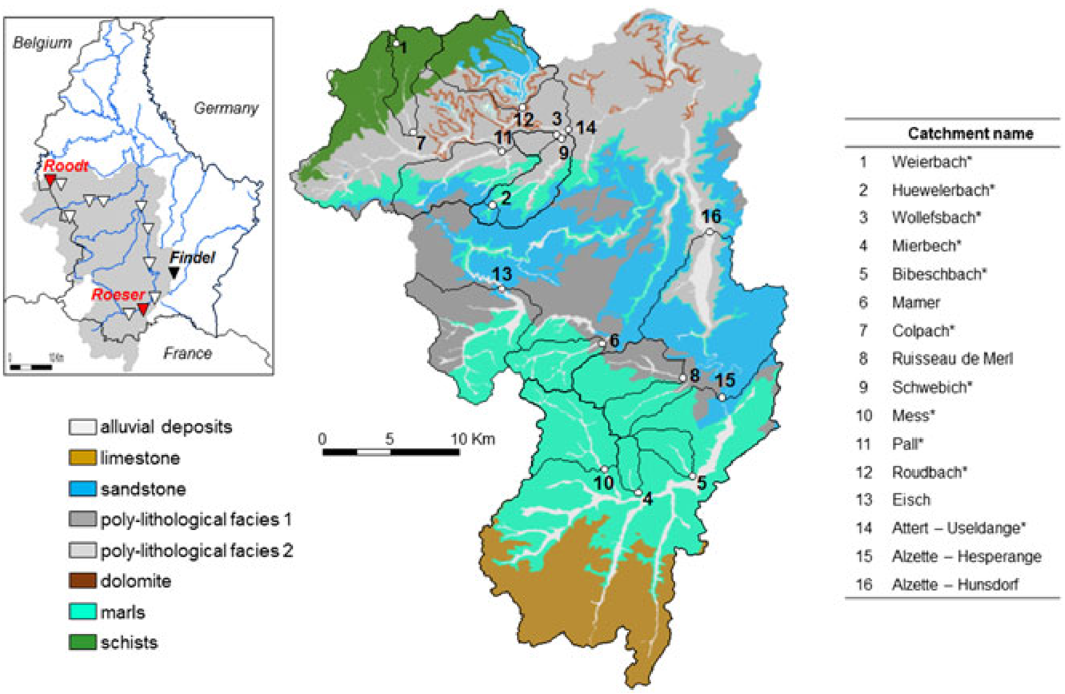

FIGURE 1 Box: map of Luxembourg, limits of the Alzette River basin (grey area), rain gauge network (reversed triangles), and precipitation sampling stations (red reversed triangles). Large map: geological map of the Alzette River basin, with nested catchments and corresponding stream gauges (white dots). The polylithological facies Category 1 covers marl and sandstone facies but is dominated by dolomitic facies. The polylithological facies Category 2 is dominated by limestone facies and includes marl and sandstone facies. Catchment names marked with an asterisk used for streamflow stable isotope data analysis. Catchment IDs ranked from the smallest to largest area

TABLE 1 Catchment mean elevation, area, percentage of bedrock geology (including subcategories of permeable [sandstone, limestone, and alluvial deposits] and impermeable [schists and marls] bedrock geology) and land use (forest, grassland, agriculture, and urban) for the 16 subcatchments

ID	Catchment	Mean elevation (m a.s.l.)	Area (km^2)	Sandstone (%)	Limestone (%)	Alluvials (%)	Permeable (%)	Schists (%)	Marls (%)	Impermeable (%)	Forest (%)	Grassland (%)	Agriculture (%)	Urban (%)	$P_{average}$ (mm)	$Q_{average}$ (mm)	$PET_{average}$ (mm)
10	Mess	324	32.2	0	0	8	8	0	92	92	9	58	23	10	746	259	620
5	Bibeschbach	298	10.4	0	0	5	5	0	95	95	48	30	15	4	742	263	624
4	Mierbech	309	6.4	0	0	4	4	0	96	96	32	16	47	5	746	233	623
13	Eisch	340	48.8	0	0	0	0	0	100	100	17	39	38	6	776	361	625
6	Mamer	333	18.0	0	0	0	0	0	100	100	5	33	44	18	747	299	625
8	Ruisseau de Merl	301	26.8	0	0	0	0	0	100	100	25	41	11	23	755	299	625
3	Wollefsbach	278	4.6	0	0	0	0	0	100	100	7	65	27	1	800	241	628
7	Colpach	442	19.2	1	5	3	9	81	10	91	51	24	23	2	970	442	598
1	Weierbach	498	0.45	0	0	0	0	100	0	31[a]	100	0	0	0	953	478	593
2	Huewelerbach	354	2.8	81	0	3	84	0	16	16	92	8	0	0	829	199	616
9	Schwebich	296	30.2	26	0	9	35	0	65	65	31	50	16	2	798	266	625
11	Pall	310	37.1	22	0	10	32	0	68	68	23	48	24	4	859	325	622
16	Alzette–Hunsdorf	318	410.1	14	28	10	52	0	48	48	31	28	17	24	751	307	625
12	Roudbach	395	43.3	27	20	3	50	37	13	50	36	27	32	5	876	336	609
15	Alzette–Hesperange	320	285.1	1	39	9	49	0	51	51	27	27	27	18	725	314	621
14	Attert–Useldange	354	249.6	12	10	7	29	24	46	70	32	35	29	4	895	423	615

Note. Catchment classification key (shaded horizontal bars) as per Figure 6: bedrock dominated by marls (light grey), schists (grey), sandstone and marls (dark grey), mixed geologies (more than three bedrock types; no shading). P = mean annual precipitation totals; Q = mean annual discharge; PET = mean annual potential evapotranspiration for the 16 subcatchments (average values for the period 2006–2014).

[a]Schistous bedrock in the Weierbach catchment is split into two categories: plateau landscapes with deep periglacial deposits and large storage capacity; hillslopes with shallow soils and small storage capacity (as per Martínez-Carreras et al., 2016).

Regosols. Their texture is mainly sandy to sandy silty. In areas dominated by marl, soils are mainly silty clayey to heavy clayey Vertisols, Planosols, Stagnosols, and Cambisols.

3 | METHODS

We used the Penman–Monteith equation (Allen, Pereira, Raes, & Smith, 1998) and the Thornthwaite (1948) method to determine potential evapotranspiration (PET) for all 16 catchments. A complete meteorological dataset required for the application of the Penman–Monteith (Allen et al., 1998) formula was only available for the Luxembourg airport station (located east of our area of interest). Because air temperature was measured in 10 stations in and around the Alzette River basin, we additionally opted for the Thornthwaite (1948) approach that only requires monthly temperature data.

We applied monthly relationships between station elevation and temperature to a 5 × 5-m digital elevation model for estimating pixel temperatures that we then averaged over the individual catchments. Next, we calculated monthly catchment PET as per Thornthwaite (1948). Finally, we disaggregated these monthly PET values into daily values, based on the number of days of each successive month of the observation period. Eventually, the difference between monthly PET data obtained via both the Penman–Monteith (at Luxembourg airport) and Thornthwaite (for each catchment) formulas was less than ±5%, demonstrating the rather negligible impact of topography on evapotranspiration compared to the large seasonal variability (annual PET values ranged from 602 to 638 mm in the Alzette basin). We did not investigate specific impacts in land use heterogeneity on evapotranspiration values.

Precipitation was measured with tipping-bucket rain gauges in 12 locations across the study catchments (Figure 1). Given that precipitation fields did not exhibit very marked topographic influences in our area of interest (tested via precipitation–rain gauge elevation relationships), we used the Thiessen polygon technique (Dingman, 1994) for generating catchment-averaged precipitation totals at daily time step.

From October 2009 to December 2014, we collected every 2 weeks grab samples of precipitation and streamflow in 11 subcatchments (Figure 1). All samples were analysed for $\delta^{18}O$ and δD using a Los Gatos DLT100 off-axis integrated cavity output spectroscopy laser spectrometer. Values are reported in per mil relative to Vienna Standard Mean Ocean Water 2 standards (International Atomic Energy Agency, 2009) with an accuracy of 0.21‰ for ^{18}O and 0.34‰ for D.

3.1 | Annual and winter precipitation–discharge ratios and average summer/winter discharge ratios

We plotted double-mass curves of precipitation versus discharge for each of the 16 catchments (as per Pfister et al., 2002). Spanning from 2006 to 2014, the slopes of the double-mass curves reflect the catchment-specific annual precipitation–discharge ratios, as well as the seasonal patterns in the rainfall–discharge transformation process. In addition, we calculated mean annual discharge, winter and annual precipitation–discharge ratios, and average summer (April–September)/winter (October–March) discharge ratios for characterising the hydrological regimes of all 16 catchments.

3.2 | Computation of catchment storage

Multiple storage metrics have been proposed in the literature, widely guided by available datasets and/or site-specific research foci. McNamara et al. (2011) insisted on the need for meaningful storage metrics in catchment comparison exercises. In this prospect, the storage–discharge relationship has been widely used as a robust descriptor of catchment behaviour (e.g., Ajami, Troch, Maddock, Meixner, & Eastoe, 2011; Creutzfeldt et al., 2014; Fenicia, Savenije, Matgen, & Pfister, 2006; Kirchner, 2009; McNamara et al., 2011; Spence, 2007). Here, we conceptualised catchment storage as a lumped metric, aggregating multiple reservoirs (e.g., soils, alluvial deposits, and regolith). We calculated daily water balance $S_{(t)}$ for the 16 study catchments:

$$\begin{aligned} S_{(t)} &= \left[R_{(t)} - Q_{(t)} - \alpha E_{(t)}\right] + S_{(t-1)} \\ &\text{if } S_{(t-1)} < 200 \text{ mm}, \alpha = S_{(t-1)}/200 \\ &\text{if } S_{(t-1)}{}^{3} > 200 \text{ mm}, \alpha = 1 \end{aligned} \tag{1}$$

where $S_{(t)}$ = catchment water balance (mm) at day t, $R_{(t)}$ = daily precipitation (mm day^{-1}), $Q_{(t)}$ = daily discharge (mm day^{-1}), $E_{(t)}$ = daily PET (mm day^{-1}), and α = weighting coefficient for limiting $E_{(t)}$ with decreasing water availability (field capacity [FC] set at 200 mm).

We computed changes in the water balance from Equation 1 at a daily time step from January 1, 2006, to December 31, 2014, for all 16 monitored catchments. For all catchments, we determined the maximum value of the water balance (S_{max}) for the 9-year observation period. We considered S_{max} as being representative of a near-complete filling of the catchment storage (as suggested by the concordant stable slopes of winter double-mass curves between aggregated precipitation and aggregated discharge in our area of interest; Pfister et al., 2002)—corresponding to a storage deficit $D_{(t)}$ close or equal to zero. Based on the S_{max} value for each catchment, we computed changes in storage deficit at a daily time step, $D_{(t)}$, as follows:

$$D_{(t)} = S_{max} - S_{(t)} \tag{2}$$

Next, we plotted logarithms of daily discharge values against daily storage deficit values for each catchment. For our catchment comparison analysis, we developed two metrics of storage deficit: (a) we used the storage deficit value corresponding to the 99th percentile of the observed flow duration curve (i.e., pronounced low-flow conditions); (b) we determined, based on an envelope line that is tangent to the hysteretic loops between daily discharge and daily storage deficit values, a hypothetical maximum storage deficit for extrapolated nearly zero-flow conditions (i.e., 0.001 mm day^{-1}).

We consider these two storage deficit metrics to implicitly inform on conceptualisations of *active storage*, S_{active}, and *total storage*, S_{total}:

1. We used the storage deficit value determined for the 99th percentile of the observed flow duration curve as a metric of an (observed) advanced depletion of soil and/or groundwater reservoirs connected to the stream. Hereafter, we refer to this storage deficit as active storage, S_{active}, that is, a measure of the observed maximum interannual variability in catchment storage.
2. We extrapolated the envelope line (tangent to the hysteretic loop between daily values of discharge and storage deficit) to nearly

zero-flow conditions (i.e., 0.001 mm day^{-1}), in order to assess a (hypothetical) absolute maximum storage deficit. We determined confidence limits for the extrapolations of the envelope line (95% confidence interval), except for catchments that run dry (allowing for a direct calculation of the absolute maximum storage deficit). Groundwater recharge (e.g., groundwater recharge from unsaturated soil drainage or perched aquifers) is considered to be negligible under these conditions (Fenicia et al., 2006). Hereafter, we refer to this (hypothetical) absolute maximum storage deficit as total storage, S_{total}, that is, a measure of the largest possible extent of catchment storage connected to the stream network.

3.3 | Precipitation and streamflow isotopic variability

We used the variability of the isotopic signatures in streamflow to define a damping ratio—expressed via the standard deviation of streamflow δD ($\sigma\delta D$). In order to limit contributions to streamflow from rapid surface or subsurface run-off generation processes, we only retained streamflow samples taken outside of rainfall events and between the 25th and 100th exceedance percentiles of the flow duration curve (see Table 3 for the number of samples retained per catchment).

We used the ratios of $\delta^{18}O$ amplitudes in streamflow and precipitation (A_S/A_P) as an additional proxy for catchment-averaged isotopic signal damping (Table 2). Amplitudes in $\delta^{18}O$ signatures in precipitation (A_P) and streamflow (A_S) were derived through sine wave curve fittings. For the streamflow-related dataset, best fits based on successive iterations were highly variable (R^2 values ranged from 0.16 to 0.51). We approximated MTT via a simple amplitude damping method (as per DeWalle, Edwards, Swistock, Aravena, & Drimmie, 1997):

$$\delta^{18}O = X + A[\cos(ct - \theta)] \tag{3}$$

where $\delta^{18}O$ is the predicted ^{18}O level (in ‰), X the annual mean measured $\delta^{18}O$ (in ‰), A the $\delta^{18}O$ annual amplitude (in ‰), c the radial frequency of annual fluctuations (0.017214 rad day^{-1}), t the time (days after start of sampling period), and θ the phase lag (in radians), and

$$T = c^{-1}\left[(A_P/A_S)^{-2} - 1\right]^{0.5} \tag{4}$$

where T is the MTT, A_P the amplitude of precipitation $\delta^{18}O$, A_S the amplitude of streamflow $\delta^{18}O$, and c the radial frequency of annual fluctuations as per Equation 3.

We used an additional approximation of a catchment's MTT by calculating the hydraulic turnover (McGuire & McDonnell, 2006), inferred from total storage and mean annual discharge:

$$T' = S_{total}/Q \tag{5}$$

Where T' is the hydraulic turnover time; S_{total} the total storage (mm), as defined in Section 3.2; and Q the mean annual discharge (mm day^{-1}).

4 | RESULTS

4.1 | Streamflow regime metrics

Over the 2006–2014 period, the monthly precipitation totals for the 16 studied catchments did not show a distinct seasonal variability

TABLE 2 Active (S_{active}) and total (S_{total}) storage, relative part of active storage, average annual discharge, median discharge, average winter precipitation–discharge ratios, average annual precipitation–discharge ratios, and average summer/winter discharge ratios for 16 catchments in the Alzette River basin (average values for the period 2006–2014)

ID	Catchment	S_{active} (mm)	S_{total} (mm)	Active storage (%)	Average discharge (mm day^{-1})	Median discharge (mm day^{-1})	R_c winter (–)	R_c annual (–)	Q_{summer}/Q_{winter} (–)
10	Mess	141	345 [304, 386]	41	0.71	0.23	0.56	0.36	0.15
5	Bibeschbach	136	154	88	0.72	0.24	0.58	0.36	0.17
4	Mierbech	107	107	100	0.64	0.12	0.53	0.32	0.06
13	Eisch	114	104 [93, 115]	100	0.99	0.37	0.72	0.47	0.20
6	Mamer	115	155 [145, 165]	74	0.82	0.24	0.62	0.41	0.16
8	Ruisseau de Merl	147	169 [143, 195]	87	0.82	0.15	0.44	0.40	0.21
3	Wollefsbach	164	237 [197, 277]	69	0.66	0.18	0.54	0.30	0.14
7	Colpach	166	203 [192, 214]	82	1.21	0.58	0.72	0.46	0.19
1	Weierbach	160	232 [225, 239]	69	1.31	0.61	0.74	0.50	0.22
2	Huewelerbach	373	1696 [1458, 1934]	22	0.52	0.45	0.25	0.25	0.73
9	Schwebich	240	1603 [1166, 2040]	15	0.73	0.30	0.47	0.33	0.27
11	Pall	200	766 [278, 1254]	26	0.89	0.47	0.54	0.38	0.28
16	Alzette–Hunsdorf	127	374 [319, 429]	34	0.84	0.59	0.54	0.42	0.44
12	Roudbach	188	374 [359, 389]	50	0.92	0.63	0.54	0.38	0.34
15	Alzette–Hesperange	151	236 [218, 254]	64	0.86	0.46	0.59	0.43	0.34
14	Attert–Useldange	155	295 [280, 310]	53	1.16	0.67	0.65	0.47	0.36

Note. For S_{total}, upper and lower 95% confidence limits given in brackets. Catchment classification key (shaded horizontal bars) as per Figure 6: bedrock dominated by marls (light grey), schists (grey), sandstone and marls (dark grey), mixed geologies (more than three bedrock types; no shading).

(Figure 2a). Average monthly precipitation for that period ranged from 60 to 80 mm, except for March, April, September (average monthly totals ranging between 30 and 50 mm), and December (average monthly total of ~110 mm).

PET for that same reference period exhibited a very pronounced seasonal variability (Figure 2b), with the smallest monthly totals (<10 mm) occurring in winter and the highest monthly totals being observed in summer (up to 120 mm). This seasonal signal in PET is mainly driven by the seasonality in temperature.

Opposite to precipitation, monthly discharge exhibited a strong seasonality, driven largely by the strong contrast in winter (October–March) and summer (April–September) PET (Figure 2c). Winter monthly discharge values were characterised by a large spread between catchments (from 20 to ~110 mm), whereas in summer the much lower monthly discharge values showed a narrow range of variability (between 5 and 15 mm).

Consequently, monthly precipitation–discharge (*Q*/*P*) ratios exhibited the highest levels (0.5 to ~0.9) in winter (December to February; Figure 2d). In certain catchments (e.g., Weierbach), monthly *Q*/*P* ratios even exceeded 1.0 (e.g., in case of delayed inflow from snowmelt—a rather marginal process in our study area—with less than 30 days with snow cover on average, 1971–2000; Pfister et al., 2005). The smallest *Q*/*P* ratios were observed in August (*Q*/*P* < 0.2 in all catchments).

Monthly PET–precipitation (*PET*/*P*) ratios were significantly lower than 1.0 in winter (October to March), suggesting that

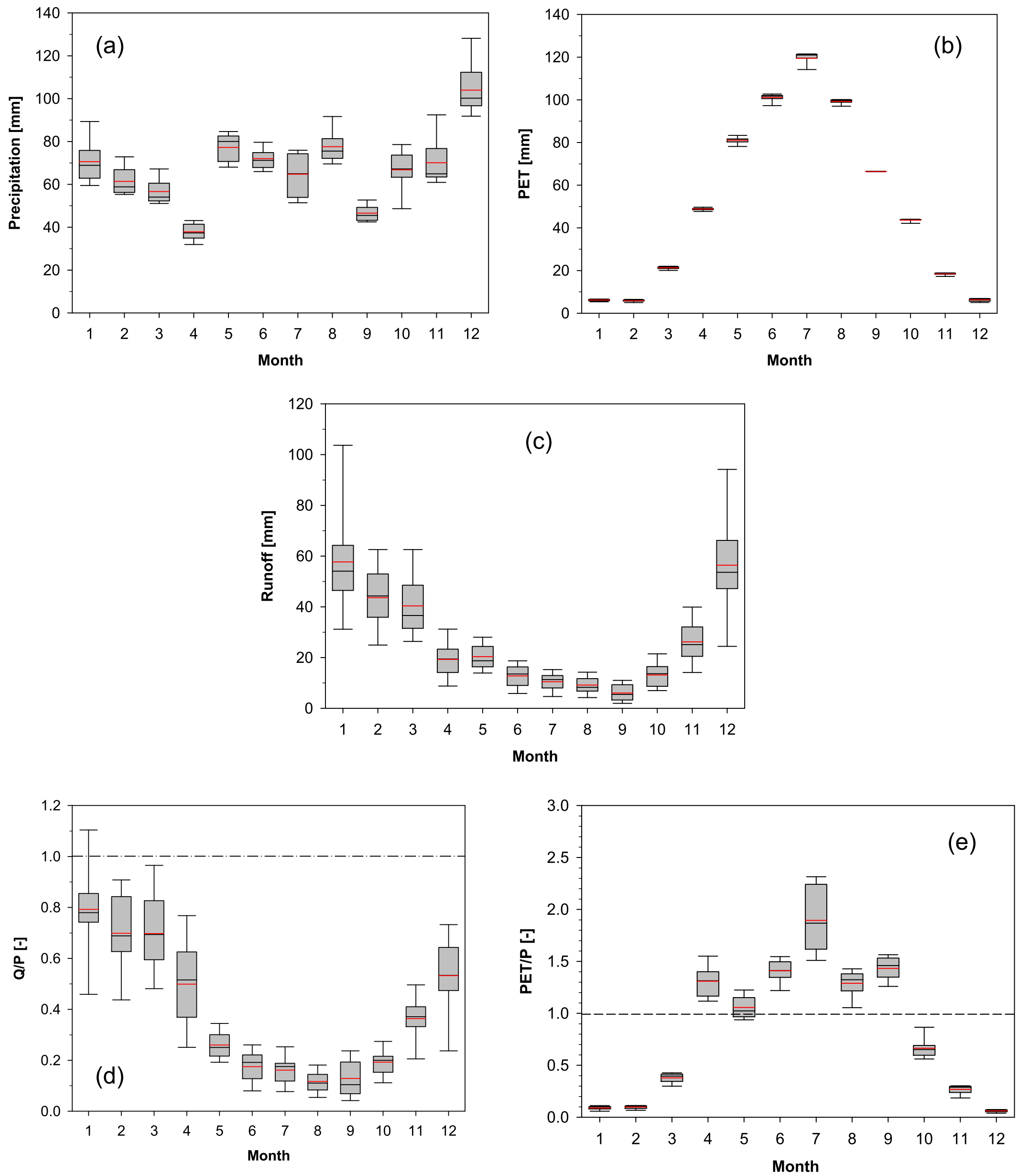

FIGURE 2 Main features of the averaged water balance components in the Alzette River basin (16 catchments; observation period 2006–2014): (a) average monthly precipitation, (b) average monthly potential evapotranspiration (PET), (c) average monthly discharge, (d) average monthly discharge–precipitation ratios, (e) average monthly PET–precipitation ratios. Box plots showing 5th/95th percentiles, average (red horizontal lines), and median values (black horizontal lines)

precipitation–discharge processes were driven mainly by precipitation during that period of the year (Figure 2e). In summer (April to September), losses through evaporation and transpiration dominated the water balance, as indicated by *PET*/*P* ratios higher than 1.0.

Double-mass curves of aggregated precipitation versus discharge (from 2006 to 2014) showed distinct patterns in the rainfall transformation into discharge across the 16 nested catchments. Catchments dominated by impermeable bedrock geology (marls and schists) exhibited large seasonal differences in this transformation process (as expressed by distinct steps in the double-mass curves; Figure 3a,b). In catchments with more permeable bedrock geology, the slopes of the double-mass curves were much flatter because of small or no seasonal differences in the transformation process (e.g., Huewelerbach catchment, Figure 3c). Larger catchments were characterised by mixed bedrock geologies and exhibited intermediate patterns in the double-mass curves between aggregated precipitation and aggregated discharge (Figure 3d).

Average annual precipitation–discharge ratios (R_c annual) in the 16 catchments ranged from 0.25 to 0.50 (Table 2). The lowest annual R_c values were found in catchments with permeable bedrock (e.g., R_c = 0.25 in the Huewelerbach, dominated by sandstone). On less permeable bedrock, the R_c values approached 0.50 (e.g., the schist-dominated Weierbach and Colpach catchments). Catchments with mixed geological substrata showed intermediate annual R_c values (e.g., Roudbach, R_c annual = 0.38).

Winter average R_c values appeared to be controlled largely by bedrock permeability (Table 2). The highest winter R_c values (up to 74% in the Weierbach) were observed in catchments dominated by more impermeable bedrock geology (i.e., marls and schists). Catchments with more than 50% of permeable bedrock geology

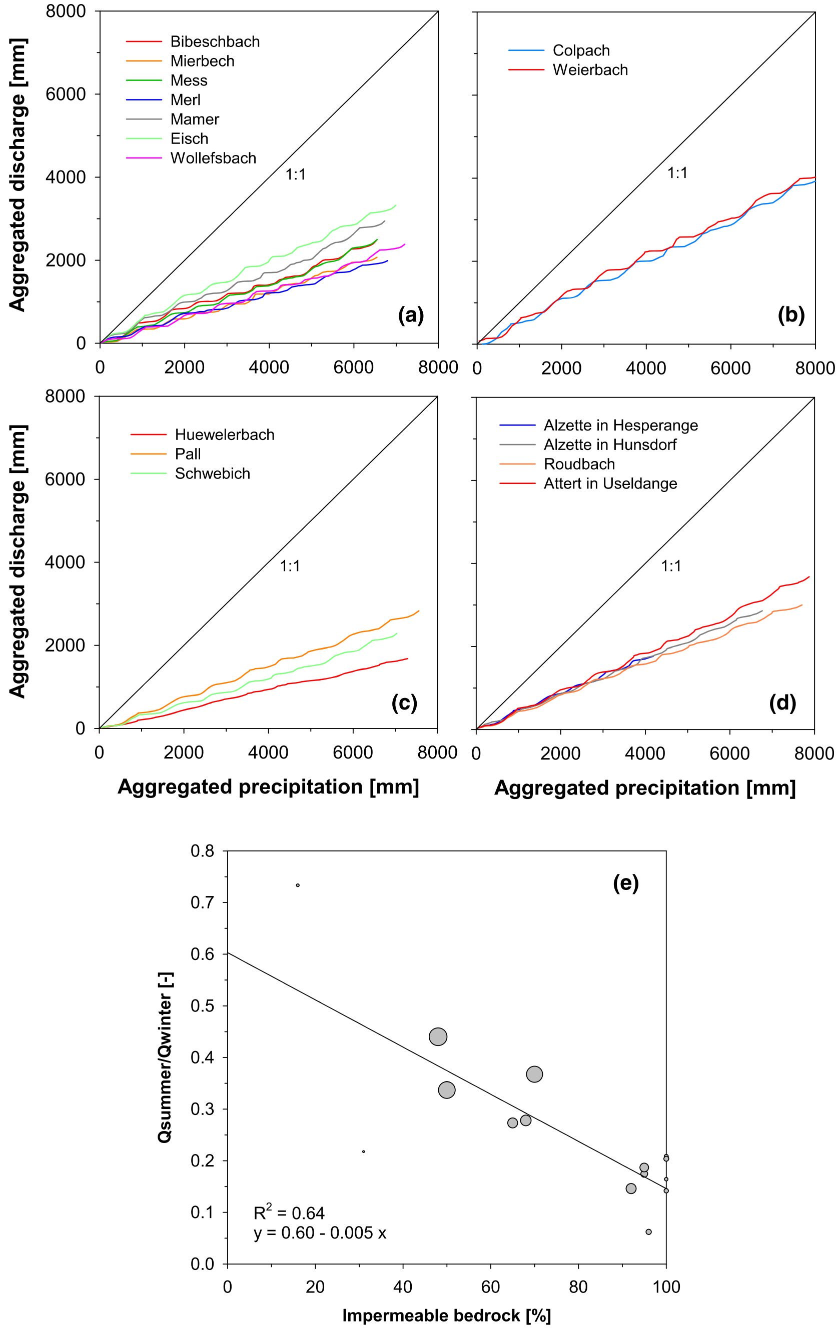

FIGURE 3 Streamflow regime metrics for 16 catchments in the Alzette River basin: double-mass curves of aggregated daily values of precipitation versus discharge in catchments with bedrock dominated by (a) marls, (b) schists, (c) sandstone and marls, and (d) mixed geologies (more than three bedrock types; period 2006–2014); (e) percentage of impermeable bedrock versus Q_{summer}/Q_{winter} ratios. Dot size proportional to log of catchment area

(i.e., sandstone, limestone, and/or alluvial deposits) exhibited the lowest winter R_c values (e.g., Huewelerbach $R_{c\ winter}$ = 0.25).

Average summer/winter discharge ratios (Q_{summer}/Q_{winter}) in the 16 catchments ranged from 0.06 to 0.73 (Figure 3e; Table 2). About 64% of the variance in Q_{summer}/Q_{winter} was explained by the percentage of impermeable bedrock (p value = .0002). We found the lowest Q_{summer}/Q_{winter} values in catchments dominated by impermeable substrates (e.g., Q_{summer}/Q_{winter} = 0.06 in the Mierbech catchment). Catchments characterised by highly impermeable bedrock exhibited Q_{summer}/Q_{winter} values below 0.3, in contrast to catchments dominated by highly permeable bedrock (e.g., Huewelerbach, Q_{summer}/Q_{winter} = 0.73).

4.2 | Catchment storage dynamics

We assessed the sensitivity of the water balance calculations (as per Equation 1) to different values of FC. Although the computed daily water balance series exhibited clear offsets for FC values of 100, 200, and 300 mm, they were not affected by any long-term increasing or decreasing trends (see example of the Roudbach catchment in Figure 4a). Annual amplitudes in the daily water balance series remained almost equal, regardless of which FC value was chosen for the calculations. Consequently, the storage deficit calculations (as per Equation 2) were mostly unaffected by the FC-induced offset in daily water balance series (Figure 4b).

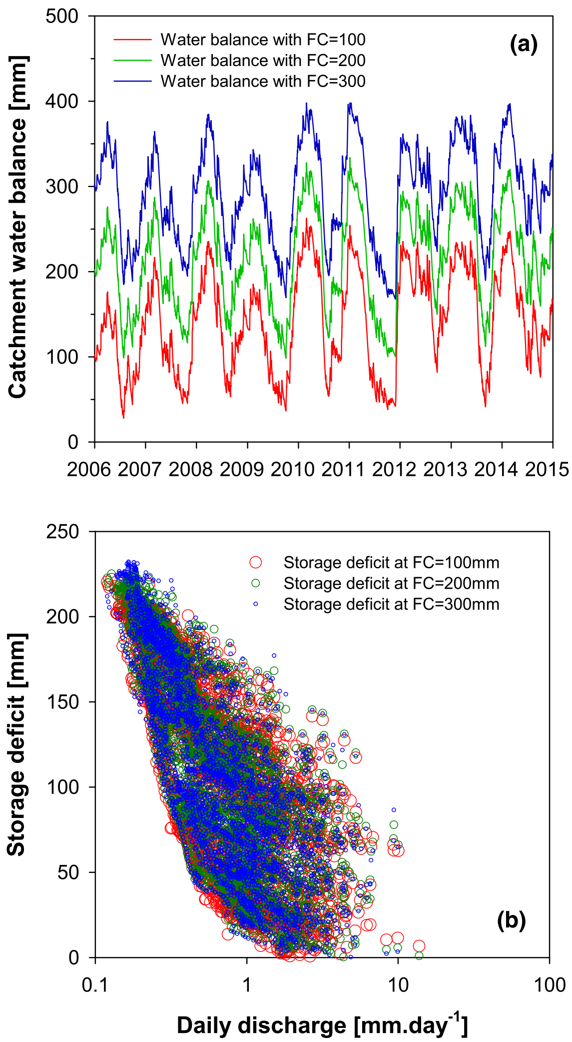

FIGURE 4 (a) Daily values of catchment water balance from 2006 to 2014 for field capacities (FCs) of 100, 200, and 300 mm. (b) Daily discharge versus daily storage deficit values for FCs of 100, 200, and 300 mm. Data from the Roudbach catchment

The daily water balances calculated for all 16 catchments showed a distinct pattern of seasonal fluctuations in catchment storage, driven mainly by precipitation inputs during winter and then by losses through evapotranspiration and groundwater depletion during summer (Figure 5).

The daily storage deficits exhibited distinct hysteretic relationships with daily discharge for our 16 catchments (Figure 6a, example of the Roudbach catchment). Consequently, a large spread in storage deficit values was observed for each individual discharge value. We also observed for each catchment a distinct lower limit in discharge for any given storage deficit value. This allowed the identification of an envelope line along the entire range of observed storage deficits and corresponding minimum discharge. This envelope line remained almost horizontal despite changes in discharge as long as storage deficit was close to zero (i.e., full saturation level) and discharge was high. The relationship gradually deviated towards the storage deficit axis with decreasing discharge (Figures 6a–e).

Whereas the (observed) active storage values (S_{active}) ranged from 107 mm (Mierbech) to 373 mm (Huewelerbach), the (estimated) total storage (S_{total}) values extended from 104 (±11) mm (Eisch) to 1696 (±238) mm (Huewelerbach; Table 2).

The fraction of active storage (S_{active}/S_{total}) ranged from ~13% (catchments dominated by permeable bedrock) to 100% (catchments dominated by schists and/or marls). S_{active}/S_{total} ratios were highest in catchments characterised by smaller total storage and subsequently less permeable bedrock (R^2 = .88, p value < .0001; Figure 7a).

4.3 | Isotope response and MTT

Isotopic signatures of D and ^{18}O in precipitation did not reveal any significant differences between the two sampling sites (Roodt and Roeser; Figure 1). Isotopic signatures in precipitation were strongly influenced by seasonal patterns in air temperature, with the largest difference in $\delta^{18}O$ between summer and winter precipitations amounting to 12‰. Given that the isotopic data series from Roodt covered a longer time span and were of higher temporal resolution, we relied on this station only for characterising input signatures in all investigated catchments.

For 11 catchments, the proxies for water mixing (i.e., standard deviations in streamflow δD and the ratio of amplitudes in ^{18}O signatures in streamflow and precipitation) were related to (active and total) storage (Table 3; Figure 7b,c). The standard deviations in streamflow δD values ranged from 0.9‰ (Huewelerbach) to 3.1‰ (Bibeschbach). The A_S/A_P ^{18}O amplitude ratios varied between 0.07 (Huewelerbach) and 0.23 (Mierbech). Both water mixing proxies exhibited the highest values in catchments characterised by small (active and total) storage levels. Active storage explained 54% (p value = .0095) and 52% (p value = .0117) of the variances in $\sigma\delta D$ and A_S/A_P ^{18}O amplitude ratios, respectively. Total storage explained 44% (p value = .027) and 46% (p value = .0217) of the variance in $\sigma\delta D$ and A_S/A_P ^{18}O amplitude ratios, respectively.

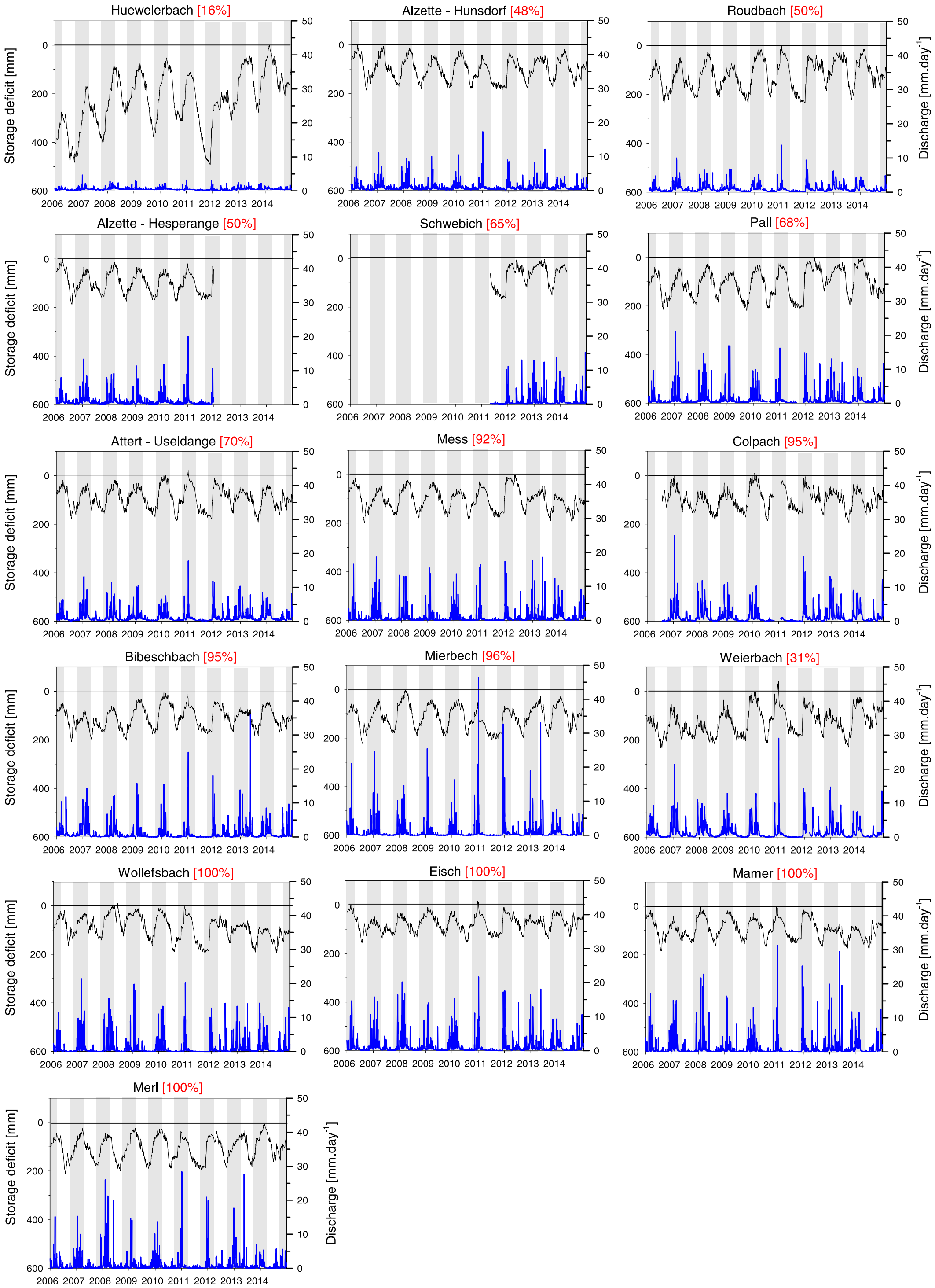

FIGURE 5 Daily storage deficit (black lines) and discharge (blue lines) for 16 catchments in the Alzette River basin (2006–2014). Percentage of impermeable bedrock next to catchment name (red characters)

Catchment MTT values approximated through the sine wave method ranged between 0.5 (catchments dominated by impermeable bedrock) and 2 years (permeable bedrock; Table 3; Figure 8a). Overall, MTT values tended to increase with higher percentages of permeable bedrock (Figure 8a,b; R^2 = .77, p value = .0004). Active storage explained 60% (p value = .0051) of the variability in catchment MTT (Figure 8b), while total storage explained 59% (p value = .0055; Figure 8b). Catchment MTT values and S_{active}/S_{total} were strongly correlated (R^2 = .55; p value = .0087; Figure 8c). Catchments exhibiting the highest S_{active}/S_{total} ratios were dominated by impermeable bedrock and were consequently characterised by low MTT values.

Catchment MTT inferred from hydraulic turnover (T) was very similar to MTT approximated by the sine wave method (T') in catchments dominated by impermeable bedrock (Table 3). In catchments dominated by permeable bedrock, the two methods gave MTT values with increasing differences. The T values plateaued at 2 years, whereas the T' values mounted up to 10 years (Table 3).

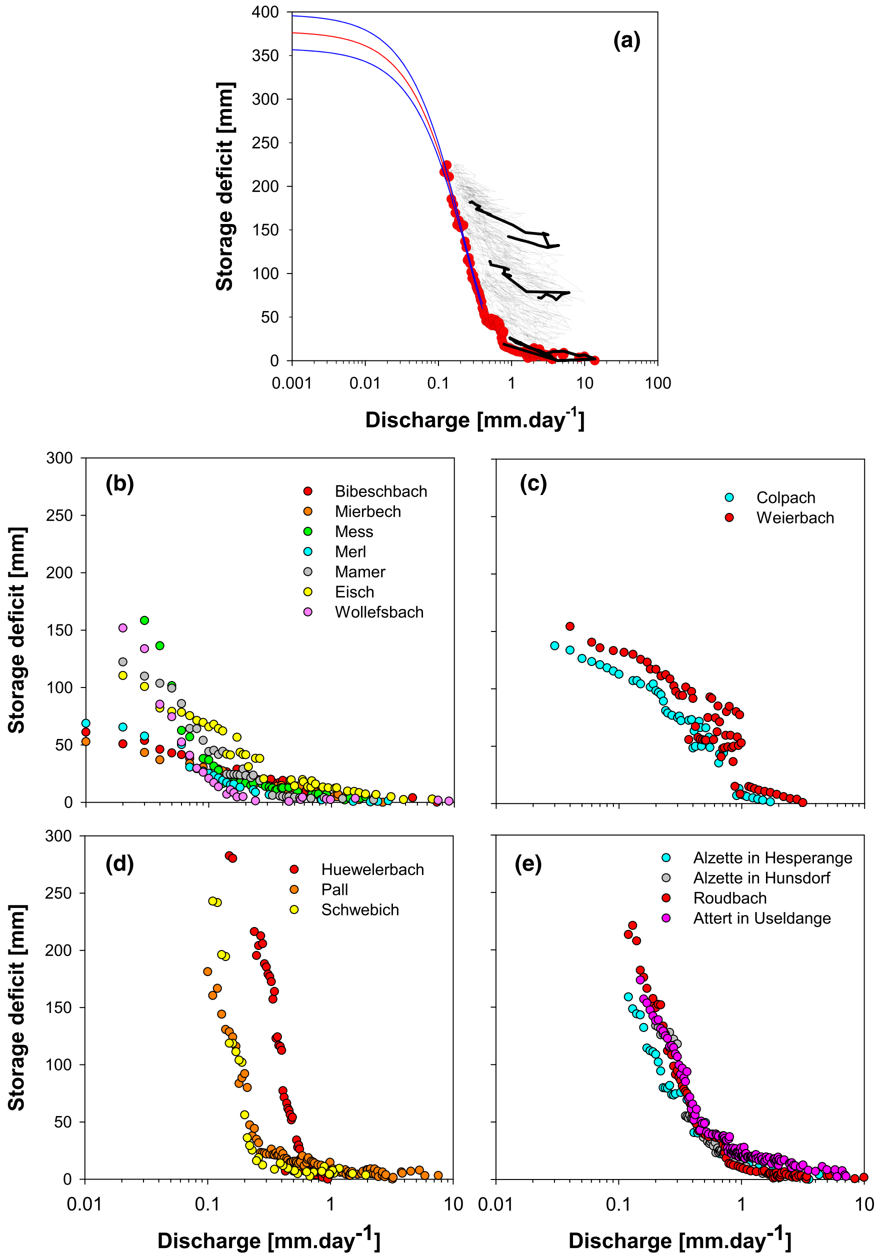

FIGURE 6 Daily discharge versus daily storage deficit: (a) example of the Roudbach catchment (grey and black lines: hysteretic loops between daily discharge and storage deficit values; red dots: envelope data; all data shown for the period 2006–2012). Discharge versus storage deficit envelope data for 16 catchments (only envelope data points shown): catchments with bedrock dominated by (b) marls, (c) schists, (d) sandstone and marls, and (e) mixed geologies (more than three bedrock types)

4.4 | Physiographic controls on water storage, mixing, and release

We investigated physiographic controls (bedrock permeability, catchment area, and land use) on water storage (expressed via S_{active} and S_{total}), release (winter and annual R_c and summer–winter discharge ratios), and mixing potential (streamflow $\sigma\delta D$, A_S/A_P ratios of ^{18}O amplitudes in streamflow and precipitation, and catchment MTT).

The correlation between forest cover percentages and bedrock geology (as expressed through percentages of impermeable bedrock) was found to be relatively high (R^2 = .51). However, for streamflow regime metrics, the correlation with forest cover percentages turned out to be rather weak (for all streamflow regime metrics, $R^2 < .25$).

In order to assess the role of catchment geology on isotopic signatures in streamflow and subsequently on catchment mixing potential, we explored the relationships between bedrock permeability, storage (S_{active} and S_{total}), streamflow $\sigma\delta D$, and A_S/A_P $\delta^{18}O$ amplitude ratios (Figures 9a–c).

Catchment bedrock permeability explained 41% (p value = 0.0074) of the variance in active storage values and 31% (p value = 0.0243) of the variance in total storage (Figure 9a). Variability in catchment mixing potential, expressed via streamflow $\sigma\delta D$ and A_S/A_P $\delta^{18}O$ amplitude ratios, appeared to be strongly related to bedrock permeability. Catchments dominated by impermeable bedrock tended to exhibit higher values in streamflow $\sigma\delta D$ and $\delta^{18}O$ A_S/A_P ratios (Figure 9b,c). The percentage of impermeable bedrock explained 70% of the variance in streamflow $\sigma\delta D$ (p value = .0014) and 62% of the variance in $\delta^{18}O$ A_S/A_P amplitude ratios (p value = .0042).

Although catchment scale explained 99% and 97% of the variance in average and maximum daily discharges, respectively (Figure 10a), the relationship between catchment scale and mixing proxies was less clear (Figure 10b). For catchments smaller than 10 km^2, streamflow $\sigma\delta D$ exhibited a large variability (0.87–2.92‰). Within the subset of

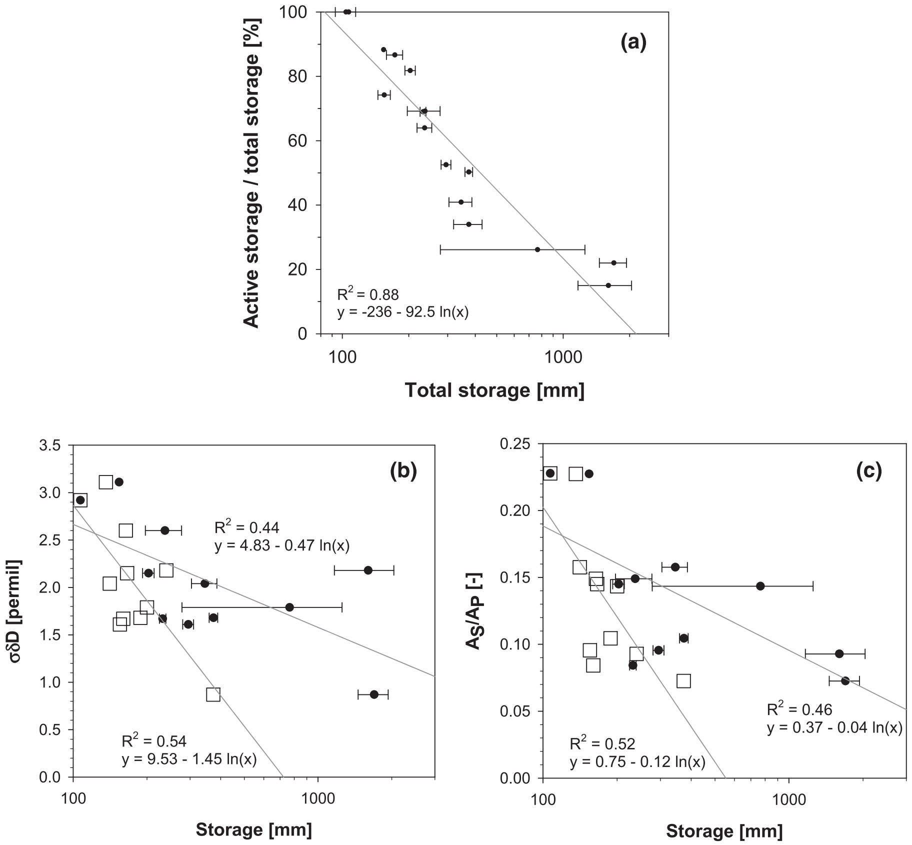

FIGURE 7 Relationships between catchment storage and streamflow isotope response: (a) percentage of active storage versus total storage (horizontal bars: upper and lower 95% confidence limits for estimated total storage); (b) catchment storage versus streamflow $\sigma\delta D$; (c) catchment storage versus ^{18}O A_S/A_P ratios. White squares represent active storage. Black dots represent total storage (with horizontal bars representing confidence limits at 95%)

TABLE 3 Number of samples retained for isotope analysis (streamflow $\sigma\delta D$ and ratio of δ^{18}O amplitudes in streamflow and precipitation), standard deviation of δD for streamflow between 25th and 100th exceedance percentiles of the flow duration curve, ratio of δ^{18}O amplitudes in streamflow and precipitation, mean transit time T (based on isotope signature damping) and T' (based on hydraulic turnover time)

ID	Catchment	Number of samples	$\sigma\delta D$ 75% (‰)	Amplitude Q/amplitude P (—)	MTT T (years)	MTT T' (years)
6	Mess	15	2.0	0.16	1.2	1.2–1.5
5	Bibeschbach	18	3.1	0.23	0.5	0.6
1	Mierbech	12	2.9	0.23	0.5	0.5
2	Eisch	n.a.	n.a.	n.a.	n.a.	0.3
3	Mamer	n.a.	n.a.	n.a.	n.a.	0.5–0.6
7	Ruisseau de Merl	n.a.	n.a.	n.a.	n.a.	0.5–0.7
10	Wollefsbach	25	2.6	0.15	0.9	0.8–1.1
11	Colpach	15	2.2	0.15	0.9	0.4–0.5
9	Weierbach	55	1.7	0.08	1.7	0.5
16	Huewelerbach	23	0.9	0.07	2.0	7.7–10.2
15	Schwebich	24	2.2	0.09	1.6	4.4–7.7
14	Pall	20	1.8	0.14	1.4	0.9–3.9
4	Alzette–Hunsdorf	n.a.	n.a.	n.a.	n.a.	1.0–1.4
13	Roudbach	24	1.7	0.10	1.4	1.1–1.2
8	Alzette–Hesperange	n.a.	n.a.	n.a.	n.a.	0.7–0.8
12	Attert–Useldange	22	1.6	0.09	1.5	0.6–0.7

Note. Catchment classification key (shaded horizontal bars) as per Figure 6: bedrock dominated by marls (light grey), schists (grey), sandstone and marls (dark grey), mixed geologies (more than three bedrock types; no shading). n.a. = not applicable.

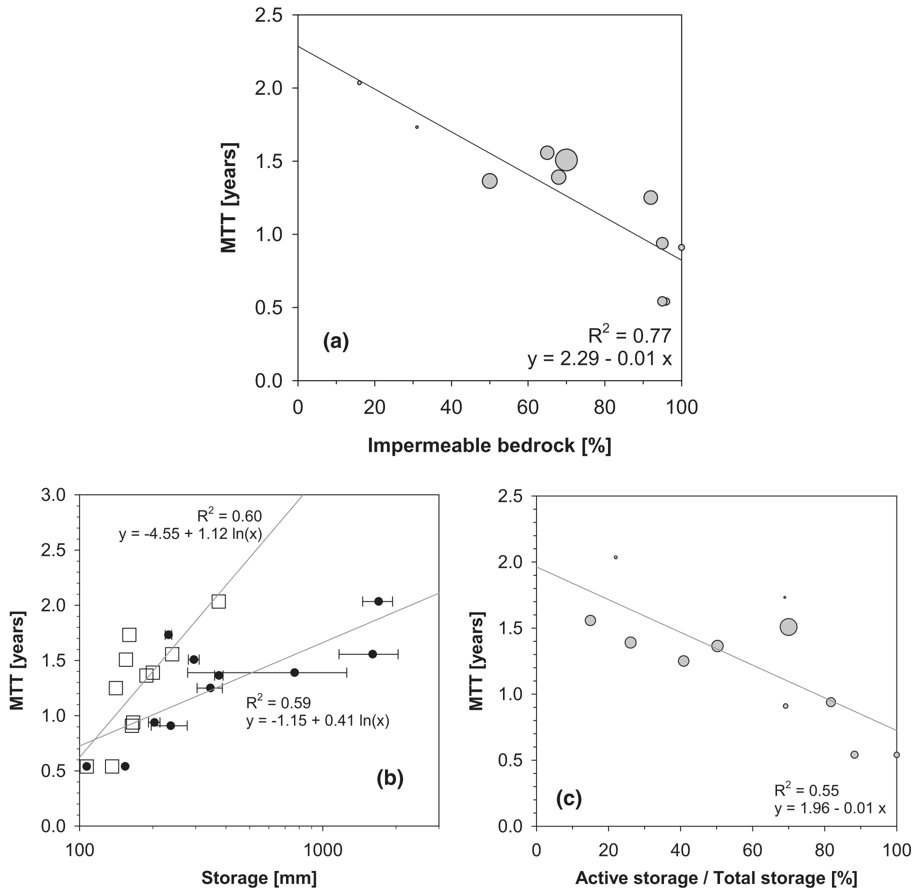

FIGURE 8 Relationships between bedrock permeability, catchment storage, and mean transit time (MTT): (a) percentage of impermeable bedrock versus catchment MTT; [b] catchment storage versus catchment MTT; (c) percentage of active storage versus catchment MTT. Dot size related to catchment area. White squares represent active storage; black dots represent total storage (with confidence limits at 95%); grey dot size proportional to logarithm of catchment area. All MTT values estimated via isotope signature damping

catchments larger than 10 km^2, $\sigma\delta D$ values appeared to gradually decrease with increasing catchment size (R^2 = .85, p value = .0005). However, it has to be noted that catchments with mixed bedrock configurations exhibited smaller $\sigma\delta D$ values, compared to catchments dominated by impermeable bedrock.

We did not find a significant relationship between land use types and storage, nor with isotopic signatures in streamflow in our set of nested catchments.

5 | DISCUSSION

5.1 | On catchment storage, isotopic signatures, and bedrock permeability

The active and total storage values determined for the catchments in our study area were significantly related to bedrock permeability. Our findings are consistent with those of Katsuyama, Ohte, and Kabeya (2005) and Uchida, McDonnell, and Asano (2006) who showed that higher bedrock permeability increased bedrock aquifer storage and discharge. Our catchments with higher bedrock permeability exhibited larger storage values and consequently had more damped high-flow peaks and lower average winter precipitation–discharge ratios (and as a corollary higher baseflow).

Tetzlaff, Seibert, McGuire, et al. (2009) have documented for diverse catchments in Scotland, United States, and Sweden that similar transit time proxies were able to document differences in flow paths and mixing processes in catchments with contrasting physiographic characteristics. In our study area, catchments with higher storage showed large mixing potential with smaller streamflow $\sigma\delta D$ values and lower A_S/A_P ^{18}O amplitude ratios. In these catchments, the response to the incoming precipitation signal was largely damped. Discharge was characterised by a rather constant and isotopically well-mixed outflow, suggesting a large groundwater reservoir. This effect was especially apparent in the sandstone-dominated Huewelerbach catchment where we observed the lowest streamflow $\sigma\delta D$ values (i.e., high mixing potential). In catchments with mixed geological conditions, our perceptual model might suggest that the large storage potential, stable low flow, and low $\sigma\delta D$ values would be dominated in winter high-flow periods by subcatchments with less permeable bedrock. Unlike permeable substrata, the latter are likely to reach their local filling maxima rapidly and eventually trigger *storage excess* behaviour—restricted to high-flow periods when they express themselves in streamflow. The schist-dominated Weierbach catchment exhibited markedly stronger isotope damping, compared to other catchments with high percentages of impermeable bedrock (i.e., marls). Extended layers of periglacial deposits and weathered schist bedrock may generate larger storage and mixing potential as

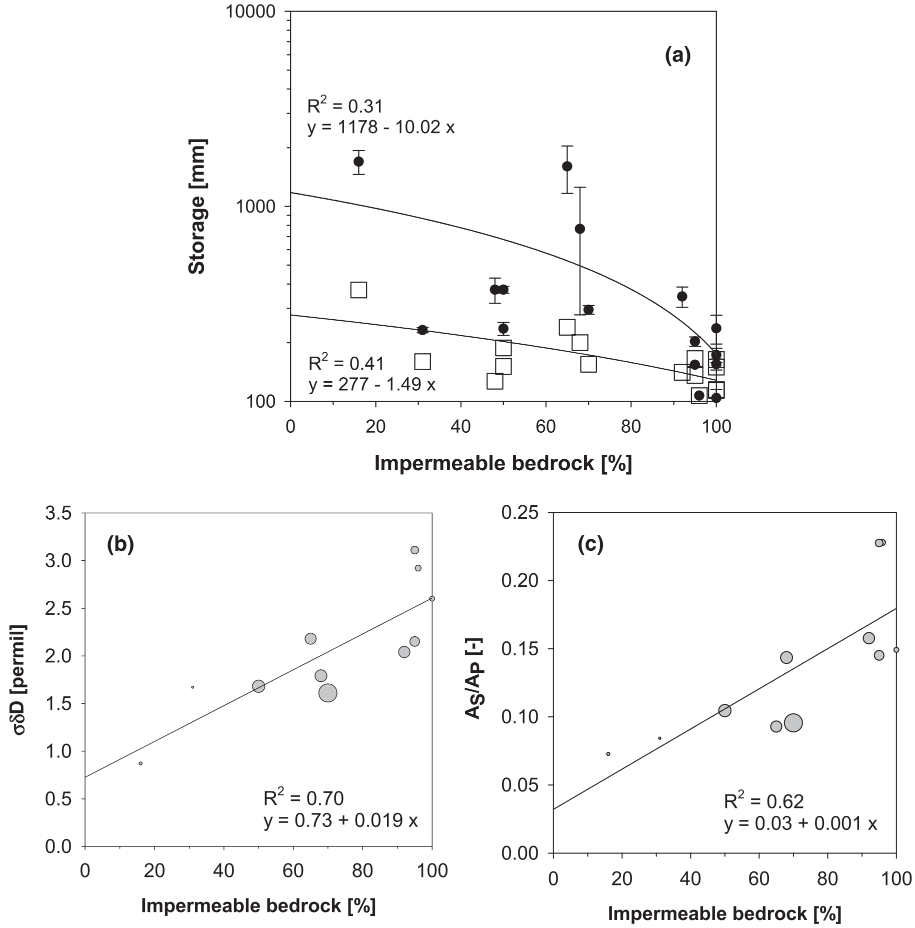

FIGURE 9 Relationships between bedrock permeability, catchment storage and streamflow isotope response: (a) percentage of impermeable bedrock versus catchment storage; (b) percentage of impermeable bedrock versus streamflow *σδD*; (c) percentage of impermeable bedrock versus $\delta^{18}O$ A_S/A_P ratios. White squares represent active storage; black dots represent total storage (with confidence limits at 95%); grey dot size proportional to logarithm of catchment area

seen in recent process work in the catchment by Martínez-Carreras et al. (2016).

Catchment MTT estimates inferred from natural tracers are likely to be highly uncertain, particularly when exceeding up to several years (DeWalle et al., 1997). Nonetheless, Soulsby, Tetzlaff, and Hrachowitz (2009) have argued that these approaches still have potential for providing first approximations of MTT and catchment-scale storage. Our estimations of catchment MTT based on the sine wave damping method ranged from 0.5 to 2 years. The heterogeneity in MTT values was greatest in catchments <20 km^2 and tended to average at ~1.4 years in larger catchments. This is consistent with findings by Soulsby et al. (2009) and Hrachowitz, Soulsby, Tetzlaff, and Speed (2009) in 32 Scottish catchments (0.5–1700 km^2), where MTT values exhibited the highest spread for catchments smaller than 10 km^2 and averaged ~2 years.

MTT values in our catchments gradually decreased with higher percentages of impermeable bedrock. Kirchner (2016) has recently demonstrated that the assumption of homogeneity in heterogeneous catchments causes strong bias in catchment MTT, leading to large underestimations of true MTT. In our study catchments, MTT was strongly correlated with storage. MTT values inferred from hydraulic turnover were significantly higher than sine-wave-based estimations in catchments dominated by permeable bedrock. This suggests that stable isotopes essentially inform contributions from active storage. In catchments with smaller $S_{\text{active}}/S_{\text{total}}$ ratios, the stable isotope information was less informative and needs to be complemented by additional tracers (e.g., tritium; Stewart, Morgenstern, McDonnell, & Pfister, 2012). Current work in the Alzette River basin is exploring the potential for tritium to provide new insights into contributions that have remained largely invisible through conventional stable-isotope-based approaches.

Finally, we observed a large spread in the storage deficit–discharge relationship for all our catchments. We have been able to delimit catchment-specific envelope lines that characterise a distinct feature of the storage deficit–discharge relationships. Along these envelope lines that are tangent to the hysteretic loops between discharge and storage deficit, discharge is solely driven by the drainage of groundwater reservoirs. Subsurface and surface run-off contribute only as storage deficits get closer to zero (and consequently discharge rapidly rises). Similar patterns in the discharge–storage relationships have been reported by Fenicia et al. (2006), McNamara et al. (2011), Creutzfeldt et al. (2014), and others. We hypothesize that the large spread in the storage deficit–discharge relationship is related to (a) the hysteresis in the event-based (mainly rainfall-driven) storage deficit–discharge relationship on the one hand and (b) the seasonal (mainly evapotranspiration-driven) change in catchment storage. The

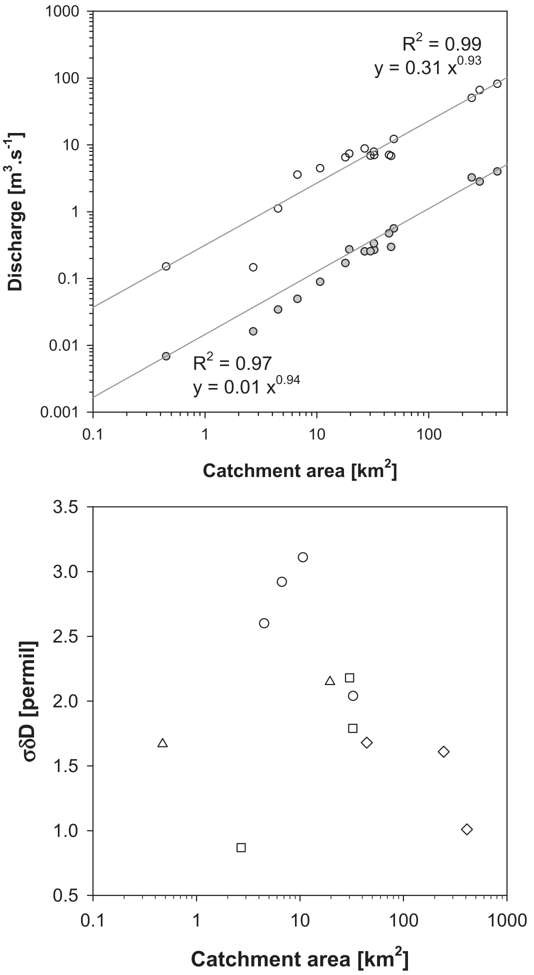

FIGURE 10 Relationships between catchment area, discharge, and streamflow isotope response: (top) catchment area versus discharge (white dots: maximum discharge; grey dots: average annual discharge); (bottom) catchment area versus streamflow $\sigma\delta D$ (circles: catchments dominated by marls; triangles: catchments dominated by schists; squares: catchments dominated by sandstone; diamonds: catchments with mixed bedrock geology)

hysteretic character of storage–flux relationships is known to be related to differences in velocities and celerities within hydrological systems (Beven, 2006; Davies & Beven, 2015). In other words, discharge depends not only on current storage but also on alternating cycles of wetting and drying. Antecedent wetness conditions are likely to influence the storage deficit profile and thereby the propagation of event perturbations (i.e., a control on celerity of the hydraulic potential through the catchment). During wetting phases, matrix storage can be bypassed through horizontal and/or vertical preferential flow paths (i.e., a control on flow velocities), as shown by Scaini et al. (2017) in the Weierbach catchment.

5.2 | On implications of our findings for catchment classification

Our findings suggest that geology is an important factor to consider for catchment classification, given its first-order effect on flow and transport. Despite the uniqueness of catchments generally (Beven, 2000) and high degree of complexity that characterises run-off response specifically (McDonnell et al., 2007), our ability to classify (and ultimately regionalise) process domains remains severely limited (McDonnell & Woods, 2004; Wagener, Sivapalan, Troch, & Woods, 2007).

Our experimental catchments with their mixed and uniform physiographic settings are good examples of how geology dominates the basic catchment functions of water collection, storage, and release (as defined by Black, 1997). Wagener et al. (2007) considered these functions to be essential components of a catchment classification system, where they are mapped onto catchment characteristics of form and hydroclimatic conditions. He, Bardossy, and Zehe (2011) note that this new generation of classification schemes has considerable potential for bringing new momentum to hydrological regionalisation.

Our data suggest that the collection (or partition) function is well expressed by winter precipitation–discharge ratios, the storage function well represented by S_{active} and S_{total}, and the release function well represented by A_S/A_P and $\sigma\delta D$. Bedrock permeability emerged as a clear and dominant control for each of these functions. These findings support the earlier hydrometric-based findings of Tague and Grant (2004) and now the ever-increasing empirical evidence of bedrock control on storage and release from headwater catchments (Capell, Tetzlaff, Hartley, & Soulsby, 2015). Hale and McDonnell (2016) showed recently that similar catchment forms and hydrologic regimes can hide very different subsurface routing, storage, and scaling behaviour—a major issue if only hydrometric data are used to define hydrological similarity for assessing land use or climate change response.

Although our findings suggest a strong control of bedrock geology on hydrological functions of water storage, mixing, and release, more research is needed for a better characterisation of catchment permeability. In our study area, Juilleret, Iffly, Hoffmann, and Hissler (2012) have recently shown the potential for soil surveys to add useful and complementary data to existing geological maps. Recent research in the schistous Weierbach catchment by Martínez-Carreras et al. (2016) has revealed the importance of two distinct landscape entities (i.e., plateaus and hillslopes) and their subsequent links to bedrock weathering and soil type (Moragues-Quiroga et al., 2017). Their seasonal interplay relative to streamflow generation imparts single- or double-peaked (delayed) storm hydrographs. Along similar lines, catchments with reportedly similar bedrock geology may well exhibit distinct precipitation–discharge transformation processes and patterns across variable scales (e.g., Katsuyama, Tani, & Nishimoto, 2010; Oda, Suzuki, Egusa, & Uchiyama, 2013; Uchida & Asano, 2010)—a feature that we have not yet been able to explore.

6 | CONCLUSION

We have presented new data from 16 nested catchments, located in a setting that covers eight distinct rock types in two geomorphic regions. Within this framework, we have assessed first-order controls on the basic catchment functions of water collection, storage, and release. We found that bedrock geology controls (a) streamflow regime metrics (as expressed by winter and annual precipitation–discharge ratios and average summer/winter discharge ratios), (b) catchment storage (storage deficit and active and total storage having been used as metrics for catchment intercomparison), and (c) isotope response (as expressed via streamflow $\sigma\delta D$, ^{18}O A_S/A_P, and catchment MTT).

The homogenous climate forcing in our region of interest allows for identifying physiographic controls on fundamental hydrological catchment functions. We have observed notable differences in stable isotope damping and MTT between catchments dominated by schist and marls (initially considered as almost equally impermeable). In order to better characterise and conceptualise subsurface characteristics (and distinguish between layers of soil, regolith, and bedrock), we are currently carrying out electrical resistivity tomography campaigns, as well as multiple soil survey campaigns, in our catchments.

Future work will also focus on controlling factors of the hysteretic relationships between catchment storage and discharge. Current hydrometric and tracer monitoring programmes in our nested catchments are to be continued and intensified for several years (thereby covering manifold configurations and sequences of drying and wetting cycles). Eventually, these datasets will serve as a backbone for concept development and testing on (time-variant) catchment (water and solute) storage and release functions.

ACKNOWLEDGMENTS

This research has received financial support through the INTER/DFG/14/02/CAOS-2 project (Catchments as organised systems) and through the FNR/CORE/C14/SR/8353440/STORE-AGE project.

We acknowledge support from L. Gourdol, J. F. Iffly, J. Juilleret, J. Frentress, and F. Barnich for their help during the sampling campaigns, sample analysis, and constructive comments. We thank L. Hopp, F. Fenicia, D. Kavetski, and P. Matgen for their helpful comments on an earlier version of this manuscript. Three anonymous referees are also acknowledged for their very constructive and helpful comments.

REFERENCES

Ajami, H., Troch, P. A., Maddock, T., Meixner, T., & Eastoe, C. (2011). Quantifying mountain block recharge by means of catchment-scale storage–discharge relationships. *Water Resources Research*, *47*, W04504. doi:10.1029/2010WR009598

Allen, R. G., Pereira, L. S., Raes, D., & Smith, M. (1998). *Crop evapotranspiration—Guidelines for computing crop water requirements*. *FAO Irrigation and Drainage Paper 56*. Food and Agriculture Organization of the United Nations: Rome, Italy.

Asano, Y., & Uchida, T. (2012). Flow path depth is the main controller of mean base flow transit times in a mountainous catchment. *Water Resources Research*, *48*, W03512. doi:10.1029/2011WR010906

Beven, K. J. (2000). Uniqueness of place and process representations in hydrological modelling. *Hydrology and Earth System Sciences*, *4*, 203–213.

Beven, K. J. (2006). Searching for the holy grail of scientific hydrology: Qt = (S, R, Δt)A as closure. *Hydrology and Earth System Sciences*, *10*, 609–618.

Black, P. E. (1997). Watershed functions. *Journal of the American Water Resources Association*, *33*, 1–11.

Botter, G., Bertuzzo, E., & Rinaldo, A. (2011). Catchment residence and travel time distributions: The master equation. *Geophysical Research Letters*, *38*, L11403. doi:10.1029/2011GL047666

Brantley, S. L., DiBiase, R. A., Russo, T. A., Shi, Y., Lin, H., Davis, K. J., … Arthur, D. K. (2016). Designing a suite of measurements to understand the critical zone. *Earth Surface Dynamics*, *4*, 211–235. doi:10.5194/esurf-4-211-2016

Buttle, J. (2016). Dynamic storage: A potential metric of inter-basin differences in storage properties. *Hydrological Processes*. doi:10.1002/hyp.10931

Capell, R., Tetzlaff, D., Malcolm, I. A., Hartley, A. J., & Soulsby, C. (2011). Using hydrochemical tracers to conceptualise hydrological function in a larger scale catchment draining contrasting geologic province. *Journal of Hydrology*, *408*, 164–177. doi:10.1016/j.jhydrol.2011.07.034

Capell, R., Tetzlaff, D., Hartley, A. J., & Soulsby, C. (2015). Linking metrics of hydrological function and transit times to landscape controls in a heterogeneous mesoscale catchment. *Hydrological Processes*, *26*, 405–420.

Carey, S. K., Tetzlaff, D., Seibert, J., Soulsby, C., Buttle, J., Laudon, H., … Pomeroy, J. W. (2010). Inter-comparison of hydro-climatic regimes across northern catchments: Synchronicity, resistance and resilience. *Hydrological Processes*, *24*, 3591–3602.

Creutzfeldt, B., Troch, P., Güntner, A., Ferré, T. P. A., Graeff, T., & Merz, B. (2014). Storage–discharge relationships at different catchment scales based on local high-precision gravimetry. *Hydrological Processes*, *28*, 1465–1475.

Davies, J. A. C., & Beven, K. (2015). Hysteresis and scale in catchment storage, flow and transport. *Hydrological Processes*, *29*, 3604–3615.

DeWalle, D. R., Edwards, P. J., Swistock, B. R., Aravena, R., & Drimmie, R. J. (1997). Seasonal isotope hydrology of three Appalachian forest catchments. *Hydrological Processes*, *11*, 1895–1906.

Didszun, J., & Uhlenbrook, S. (2008). Scaling of dominant runoff generation processes: Nested catchments approach using multiple tracers. *Water Resources Research*, *44*, . doi:10.1029/2006WR005242

Dingman, L. (1994). *Physical hydrology*. Prentice Hall: Englewood Cliffs, New Jersey.

FAO-ISRIC-IUSS (2006). *World reference base for soil resources 2006*. *World Soil Resources Reports 103* (pp. 128). Rome: Food and Agriculture Organisation.

Fenicia, F., Savenije, H. H. G., Matgen, P., & Pfister, L. (2006). Is the groundwater reservoir linear? Learning from data in hydrological modelling. *Hydrology and Earth System Sciences*, *10*, 139–150.

Fröhlich, H. L., Breuer, L., Vaché, K. B., & Frede, H. G. (2008). Inferring the effect of catchment complexity on mesoscale hydrologic response. *Water Resources Research*, *44*, W09414. doi:10.1029/2007WR006207

Hale, C., & McDonnell, J. J. (2016). Effect of bedrock permeability on stream base flow mean transit time scaling relations: 1. A multiscale catchment intercomparison. *Water Resources Research*, *52*, 1358–1374. doi:10.1002/2014WR016124

Haria, A. H., & Shand, P. (2004). Evidence for deep sub-surface flow routing in forested upland Wales: Implications for contaminant transport and stream flow generation. *Hydrology and Earth System Sciences*, *8*, 334–344.

He, Y., Bardossy, A., & Zehe, E. (2011). A review of regionalisation for continuous streamflow simulation. *Hydrology and Earth System Sciences*, *15*, 3539–3553.

Hrachowitz, M., Soulsby, C., Tetzlaff, D., Dawson, J. J. C., & Malcolm, I. A. (2009). Regionalisation of transit time estimates in montane catchments by integrating landscape controls. *Water Resources Research*, *45*, W05421. doi:10.1029/2008WR004496

Hrachowitz, M., Soulsby, C., Tetzlaff, D., & Speed, M. (2009). Catchment transit times and landscape controls—Does scale matter? *Hydrological Processes*, *24*, 117–125. doi:10.1002/hyp.7510

IAEA. 2009. Reference sheet for international measurement standards—VSMOW2 & SLAP2 (issue date: 5 May 2009).

Jencso, K. G., McGlynn, B. L., Gooseff, M. N., Wondzell, S. M., Bencala, K. E., & Marshall, L. A. (2009). Hydrologic connectivity between landscapes and streams: Transferring reach- and plot-scale understanding to the catchment scale. *Water Resources Research*, *45*, W04428. doi:10.1029/2008WR007225

Juilleret, J., Iffly, J. F., Pfister, L., & Hissler, C. (2011). Remarkable Pleistocene slope deposits in Luxembourg (Oesling): Pedological implication and geosite potential. *Bulletin de la société des naturalistes luxembourgeois*, *112*, 125–130.

Juilleret, J., Iffly, J. F., Hoffmann, L., & Hissler, C. (2012). The potential of soil survey as a tool for surface geological mapping: A case study in a hydrological experimental catchment (Huewelerbach, Grand-Duchy of Luxembourg). *Geologica Belgica*, *15*, 36–41.

Katsuyama, M., Ohte, N., & Kabeya, N. (2005). Effects of bedrock permeability on hillslope and riparian groundwater dynamics in a weathered granite catchment. *Water Resources Research*, *41*, W01010. doi:10.1029/2004WR003275

Katsuyama, M., Tani, M., & Nishimoto, S. (2010). Connection between streamwater mean residence time and bedrock groundwater recharge/discharge dynamics in weathered granite catchments. *Hydrological Processes*, *24*, 2287–2299. doi:10.1002/hyp.7741

Kirchner, J. (2009). Catchments as simple dynamical systems: Catchment characterization, rainfall-runoff modeling, and doing hydrology backward. *Water Resources Research*, *45*, W02429. doi:10.1029/2008WR006912

Kirchner, J. W. (2016). Aggregation in environmental systems: Catchment mean transit times and young water fractions under hydrologic nonstationarity. *Hydrology and Earth System Sciences*, *20*, 299–328.

Klaus, J., Chun, K. P., McGuire, K. J., & McDonnell, J. J. (2015). Temporal dynamics of catchment transit times from stable isotope data. *Water Resources Research*, *51*, 4208–4223. doi:10.1002/2014WR016247

Kosugi, K., Katsura, S., Katsuyama, M., & Mizuyama, T. (2006). Water flow processes in weathered granitic bedrock and their effects on runoff generation in a small headwater catchment. *Water Resources Research*, *42*, W02414. doi:10.1029/2005WR004275

Martínez-Carreras, N., Hissler, C., Gourdol, L., Klaus, J., Juilleret, J., Iffly, J. F., & Pfister, L. (2016). Storage controls on the generation of double peak hydrographs in a forested headwater catchment. *Journal of Hydrology*, *543*, 255–269. doi:10.1016/j.jhydrol.2016.10.004

McDonnell, J. J., & Beven, K. (2014). Debates—The future of hydrological sciences: A (common) path forward? A call to action aimed at understanding velocities, celerities and residence time distributions of the headwater hydrograph. *Water Resources Research*, *50*, 5342–5350. doi:10.1002/2013WR015141

McDonnell, J. J., & Woods, R. (2004). On the need for catchment classification. *Journal of Hydrology*, *299*, 2–3.

McDonnell, J. J., Sivapalan, M., Vaché, K., Dunn, S., Grant, G., Haggerty, R., … Weiler, M. (2007). Moving beyond heterogeneity and process complexity: A new vision for watershed hydrology. *Water Resources Research*, *43*, W07301. doi:10.1029/2006WR005467

McGuire, K. J., & McDonnell, J. J. (2006). A review and evaluation of catchment transit time modelling. *Journal of Hydrology*, *330*, 543–563.

McGuire, K. J., & McDonnell, J. J. (2010). Hydrological connectivity of hillslopes and streams: Characteristic time scales and nonlinearities. *Water Resources Research*, *46*, W10543. doi:10.1029/2010WR009341

McGuire, K. J., McDonnell, J. J., Weiler, M., Kendall, C., McGlynn, B. L., Welker, J. M., & Seibert, J. (2005). The role of topography on catchment-scale water residence time. *Water Resources Research*, *41*, W05002. doi:10.1029/2004WR003657

McNamara, J. P., Tetzlaff, D., Bishop, K., Soulsby, C., Seyfried, M., Peters, N. E., … Hooper, R. (2011). Storage as a metric of catchment comparison. *Hydrological Processes*, *25*, 3364–3371.

Montgomery, D. R., Dietrich, W. E., Torres, R., Anderson, S. P., Heffner, J. T., & Loague, K. (1997). Hydrologic response of a steep, unchanneled valley to natural and applied rainfall. *Water Resources Research*, *33*, 91–109.

Moragues-Quiroga, C., Juilleret, J., Gourdol, L., Pelt, E., Perrone, T., Aubert, A., … Hissler, C. (2017). Genesis and evolution of regoliths: Evidence from trace and major elements and Sr–Nd–Pb–U isotopes. *Catena*, *149*, 185–198. doi:10.1016/j.catena.2016.09.015

Oda, T., Suzuki, M., Egusa, T., & Uchiyama, Y. (2013). Effect of bedrock flow on catchment rainfall–runoff characteristics and the water balance in forested catchments in Tanzawa Mountains, Japan. *Hydrological Processes*, *27*, 3864–3872. doi:10.1002/hyp.9497

Onda, Y., Komatsu, Y., Tsujimura, M., & Fujihara, J. (2001). The role of subsurface runoff through bedrock on storm flow generation. *Hydrological Processes*, *15*, 1693–1706.

Pfister, L., Iffly, J. F., El Idrissi, A., & Hoffmann, L. (2000). Définition de zones hydrologiquement homogènes au Grand-duché de Luxembourg sur base de critères physiogéographiques en vue d'opérations de régionalisation. *Archives de l'Institut grand-ducal de Luxembourg—Section des Sciences naturelles, physiques et mathématiques*, *43*, 239–253.

Pfister, L., Humbert, J., & Hoffmann, L. (2000). Recent trends in rainfall–runoff characteristics in the Alzette River basin, Luxembourg. *Climatic Change*, *45*, 323–337.

Pfister, L., Iffly, J. F., Hoffmann, L., & Humbert, J. (2002). Use of regionalized stormflow coefficients with a view to hydroclimatological hazard mapping. *Hydrological Sciences Journal*, *47*(3), 479–491.

Pfister, L., Wagner, C., Vansuypeene, E., Drogue, G., & Hoffmann, L. (2005). In C. Ries (Ed.), *Atlas climatique du grand-duché de Luxembourg*). Luxembourg: Musée National d'Histoire Naturelle, Société des naturalistes luxembourgeois, Centre de Recherche Public—Gabriel Lippmann, Administration des Services Techniques de l'Agriculture.

Rinaldo, A., Benettin, P., Harman, C. J., Hrachowitz, M., McGuire, K. J., van der Velde, Y., … Botter, G. (2015). Storage selection functions: A coherent framework for quantifying how catchments store and release water and solutes. *Water Resources Research*, *51*, 4840–4847. doi:10.1002/2015WR017273

Sayama, T., McDonnell, J. J., Dhakal, A., & Sullivan, K. (2011). How much water can a watershed store ? *Hydrological Processes*, *25*, 3899–3908.

Scaini, A., Audebert, M., Hissler, C., Fenicia, F., Gourdol, L., Pfister, L., & Beven, K. J. (2017). Velocity and celerity dynamics at plot scale inferred from artificial tracing experiments and time-lapse ERT. *Journal of Hydrology*, *546*, 28–43. doi:10.1016/j.jhydrol.2016.12.035

Smakhtin, V. U. (2001). Low flow hydrology: A review. *Journal of Hydrology*, *240*, 147–186.

Soulsby, C., Tetzlaff, D., Rodgers, P., Dunn, S., & Waldron, S. (2006). Runoff processes, streamwater residence times and controlling landscape characteristics in a mesoscale catchment: An initial evaluation. *Journal of Hydrology*, *325*, 197–221.

Soulsby, C., Tetzlaff, D., & Hrachowitz, M. (2009). Tracers and transit times: Windows for viewing catchment scale storage? *Hydrological Processes*, *23*, 3503–3507.

Spence, C. (2007). On the relation between dynamic storage and runoff: A discussion on thresholds, efficiency, and function. *Water Resources Research*, *43*, W12416. doi:10.1029/2006WR005645

Spence, C. (2010). A paradigm shift in hydrology: Storage thresholds across scales influence catchment runoff generation. *Geography Compass*, *4*(7), 819–833. doi:10.1111/j.1749-8198.2010.00341.x

Stewart, M. K., Morgenstern, U., McDonnell, J. J., & Pfister, L. (2012). The “hidden streamflow” challenge in catchment hydrology: A call to action for stream water transit time analysis. *Hydrological Processes*, *26*, 2061–2066.

Tague, C., & Grant, G. E. (2004). A geological framework for interpreting the low-flow regimes of Cascade streams, Willamette River Basin, Oregon. *Water Resources Research*, *40*, W04303. doi:10.1029/2003WR002629

Tetzlaff, D., Seibert, J., McGuire, K. J., Laudon, H., Burns, D. A., Dunn, S. M., & Soulsby, C. (2009). How does landscape structure influence catchment transit time across different geomorphic provinces? *Hydrological Processes*, *23*, 945–953.

Tetzlaff, D., Seibert, J., & Soulsby, C. (2009). Inter-catchment comparison to assess the influence of topography and soils on catchment transit times in a geomorphic province; The Cairngorm mountains, Scotland. *Hydrological Processes*, *23*, 1874–1886.

Tetzlaff, D., McNamara, J., & Carey, S. K. (2011). Measurements and modelling of storage dynamics across scales. *Hydrological Processes*, *25*, 3831–3835. doi:10.1002/hyp.8396

Thornthwaite, C. W. (1948). An approach toward a rational classification of climate. *Geographical Review*, *38*, 55–94.

Troch, P., Durcik, M., Seneviratne, S. I., Hirschi, M., Teuling, A. J., Hurkmans, R., & Hasan, S. (2007). New data sets to estimate terrestrial water storage change. *Eos Transactions AGU*, *88*(45), 469–470.

Uchida, T., & Asano, Y. (2010). Spatial variability in the flowpath of hillslope runoff and streamflow in a meso-scale catchment. *Hydrological Processes*, *24*, 2277–2286. doi:10.1002/hyp.7767

Uchida, T., McDonnell, J. J., & Asano, Y. (2006). Functional intercomparison of hillslopes and small catchments by examining water source, flowpath and mean residence time. *Journal of Hydrology*, *327*, 627–642.

Viville, D., Ladouche, B., & Bariac, T. (2006). Isotope hydrological study of mean transit time in the granitic Strengbach catchment (Vosges massif, France): Application of the FlowPC model with modified input function. *Hydrological Processes*, *20*, 1737–1751.

Wagener, T., Sivapalan, M., Troch, P., & Woods, R. (2007). Catchment classification and hydrologic similarity. *Geography Compass*, *1*(4), 901–931.

Wrede, S., Fenicia, F., Martínez-Carreras, N., Juilleret, J., Hissler, C., Krein, A., … Pfister, L. (2015). Towards more systematic perceptual model development: A case study using 3 Luxembourgish catchments. *Hydrological Processes*, *29*, 2731–2750. doi:10.1002/hyp.10393

How to cite this article: Pfister L, Martínez-Carreras N, Hissler C, et al. Bedrock geology controls on catchment storage, mixing, and release: A comparative analysis of 16 nested catchments. *Hydrological Processes*. 2017;31:1828–1845. https://doi.org/10.1002/hyp.11134